Coil Dimensions of Polystyrene Chains in Colloid−Polymer Mixtures at the Protein Limit: A SANS Study

Thomas Kramer, Ralf Schweins,† and Klaus Huber*

Fakultät für Naturwissenschaften, Department Chemie, Universität Paderborn, Warburger Str. 100, D-33098 Paderborn, Germany

Received June 21, 2005; Revised Manuscript Received September 7, 2005

ABSTRACT: A new combination of polymer chains and small colloids is presented in order to investigate the behavior of colloid−polymer mixtures in solution (CP) in the protein limit. To this end, hydroxy-functionalized silica particles (OHSil) were prepared according to a procedure [*J. Am. Chem. Soc.* **2003**, *125*, 3712], which led to colloid radii as small as 1.2 nm. Compared to this small size, the coil dimensions of the polystyrene (PS) chains used as the polymer component were larger by more than an order of magnitude. Investigation of the CP focused on the dimension of the PS chains in the presence of a varying amount of OHSil colloids. Chain size and shape were characterized by means of light scattering, viscosity experiments, and small-angle neutron scattering (SANS). Two solvents have been used. A mixture of dimethylformamide (DMF) with toluene was isorefractive to the OHSil particles, giving access to single chain behavior of PS. Pure DMF, on the other hand, allowed an efficient contrast matching of OHSil suitable for SANS experiments on fully deuterated PS. All characterization techniques provided clear evidence for a shrinking of the coil dimensions with increasing OHSil content in the solution. Particle scattering factors from SANS yielded a detailed picture of this chain compaction. The smallest coil dimensions were recorded close to the liquid−liquid phase boundary, occurring at an OHSil volume fraction of ∼0.17. This is considered to be a first experimental evidence for a shift of the liquid−liquid phase boundary toward lower colloid volume fractions if the colloid size increases. Altogether, present data extend earlier measurements on two chemically different CP in the protein limit, thus establishing the observed shrinking to be a universally valid feature of these systems. The results are in qualitative agreement with theoretical predictions.

Introduction

Interest in mixtures of polymer chains and colloidal particles (CP) in solution dates back to the pioneering work of Oosawa and Asakura[1] and Vrij.[2] They theoretically investigated hard spheres mixed with small polymeric chains and found a depletion interaction among the large colloidal spheres. Since then, theoretical knowledge and experimental evidence were significantly broadened.[3,4] Within this field an interesting topic emerged, which focused on CP mixtures with small colloidal particles dissolved together with much larger polymer chains.

The latter case established the so-called protein limit.[4] Frequently occurring systems in nature and in biochemical applications are responsible for an ever-growing scientific interest in such systems. Usually, small globular proteins coexist in the presence of large polymeric chains lending the name to this type of CP mixture. Examples are the microcompartmentation in the cytoplasma[5] caused by a subtle interplay of various biopolymeric components, DNA compaction in the cytoplasma of bacteria,[6] and potential instability of large exocellular polysaccharides produced during the fermentation process of milk in the presence of small proteins.[7]

One of the first theoretical treatments of CP mixtures in the protein limit has been performed by de Gennes,[8] who calculated the change in free energy while immersing a small colloidal particle into a large polymer chain. He found a decrease of this free energy change with increasing size R_g of the polymer chain causing extensive miscibility of CP in the protein limit unlike the phase instability of CP mixtures with the inverse size ratio.[3,4] However, this miscibility regime seems to diminish[9,10] if the solvent quality worsens for the polymeric component. Along with the phase separation,[9,10] depletion interactions among the small colloids and polymer segments also cause a shrinking of the polymer coil dimensions[11−15]—in partial analogy to the coil collapse of polymers in Θ-solvents if the phase boundary is approached. The theoretical effort[15] to interpret the osmotic compaction of DNA into a nucleoid by means of interactions between globular proteins and supercoiled DNA is in close relation to this feature. These theoretical predictions can be tested by computer simulations or by experiments.

Computer simulations of both the phase behavior[16] and the chain conformation[17,18] in fact agree with the above-mentioned theoretical predictions. The latter[17,18] were performed on cubic-lattice chains in a vacuum, representing athermal conditions. The focus lay on changes of the coil dimensions, induced by the addition of "solvent particles", which are considered to represent small colloids. In the presence of a significant and constant volume fraction of "solvent particles", the exponent of a plot of coil size vs the degree of polymerization decreased from 0.58 in a vacuum to 0.34, indicating a full collapse of the coils.[17] The process of coil shrinking could be followed by gradually increasing the amount of solvent particles.[18] In a more recent paper, simulations were extended to include semidilute polymer solutions and interaction energies among the different components.[19]

† Institut Laue-Langevin, LSS Group, B.P. 156, 6 rue Jules Horowitz, F-38042, Grenoble CEDEX 9, France.

* Corresponding author: e-mail klaus.huber@upb.de; Ph +49-5251-602125; Fax +49-5251-604208.

10.1021/ma051308j CCC: $30.25
Published on Web 10/22/2005

Experiments on CP in the protein limit are much more scarce and until recently were confined to the colloid−colloid interaction and the phase behavior.[7] The biggest hurdle which had to be overcome was to generate appropriate model systems. Such systems should include monodisperse polymer chains and colloids which allow for an investigation of either component in the presence of the other component, respectively. In addition, the colloids have to be as close to the spherical shape as possible and small enough in order to establish the protein limit. In our preceding work,[20−22] we developed two systems, which at least partly fulfilled the requirements and led to first structural results of polymer chains in CP mixtures in the protein limit.

In one system,[20,21] large polystyrene (PS) chains were mixed with poly(ethyl methacrylate) (PEMA) colloids. The PEMA colloids had a radius R_C of 13 nm, which was significantly smaller than the radius of gyration R_g of the PS chains corresponding to $6 < R_g/R_C < 9$. Their refractive index was matched in toluene, thus facilitating light scattering (LS) investigations of the coexisting PS chains. Unfortunately, a slight degree of mismatch excluded an interpretation of scattering results in terms of a single chain behavior beyond 2 wt % of the colloid content, and below this content, the PEMA colloids did not affect the size of the polymer chains.[20] To extend structural research toward higher colloid contents, small-angle neutron scattering (SANS) was performed on deuterated PS chains in the same system. Investigation of the scattering curves at PEMA colloid contents c_C covering a regime of 0 g/L $< c_C <$ 201 g/L indicated a compaction of the PS chains to half of its original size.[21]

Suppression of the scattering contrast for LS experiments could be improved with a second system.[22] On the basis of the idea to use octa-*n*-propylsilsesquioxane (SILS) molecules as the colloidal component, we were able to generate a CP mixture with homodisperse colloidal particles leading to an extremely large value of $R_g/R_C > 20$. At the same time, interpretation of light scattering experiments in terms of single PS chain behavior became possible up to $c_C \sim 200$ g/L in the mixed solvent toluene−ethyl acetate, which was isorefractive to SILS. Higher SILS contents were not accessible due to an insolubility of SILS. Extension of c_C was achieved in pure toluene, but in pure toluene we had to rely on viscosity measurements due to a mismatch of the scattering contrast of the SILS particles. By means of viscosity experiments and light scattering, a collapse concentration of $c_C \sim 500$ g/L could be located via extrapolating available data. Results from both solvents provide first experimental evidence for a shrinking of the coil dimensions in good solvents induced by the addition of small colloids, in line with theoretical predictions. In addition, we succeeded to confirm the narrowing of the stability regime of CP mixtures in the protein limit if the solvent conditions were changed from "good" to "Θ".[22]

However, synthetic colloid components in the protein limit suffer from an intrinsic problem. Because of the fact that colloids smaller than 10 nm approach the size of conventional molecules, their specific chemical nature may play a more important role than it does in the case of large colloids having diameters of 100 nm and more. Beyond this chemical differentiation, very small colloids are more prone to irregularities in size and shape than large regularly shaped compact, spherelike colloid particles are. Thus, we are still far from being able to raise trends observed with PS/PEMA and PS/SILS to universally valid principles of CP in the protein limit.

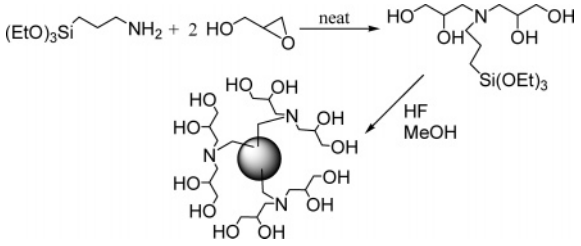

Figure 1. Schematic presentation of the OHSil synthesis.

To confirm the observed behavior and to put it on a broader body of evidence, we looked for an alternative colloid component, suitable to be combined with PS chains. The choice fell on hydroxy-functionalized silica particles, denoted as OHSil. The system was recently introduced by Mori et al.[23] Compared to the two colloid components used in the preceding work,[20−22] it provides the following advantages: (i) the OHSil colloids are only slightly larger than the SILS particles,[22] thus still giving rise to values of $R_g/R_c \gg 1$, yet being more like a typical colloid than SILS; (ii) OHSil particles are smaller and less prone to a swelling under good solvent conditions than are PEMA particles.[20,21] With this in mind, dilute solution behavior of PS chains is investigated by means of LS and viscosity measurements in the presence of varying amounts of OHSil colloids. The colloid concentration c_C covers a regime of $0 \leq c_C \leq 105$ g/L. Experiments were performed in two different solvents, dimethylformamide (DMF) and a mixture of DMF and toluene, the latter being approximately isorefractive to the OHSil particles. Both solvents act as good solvents for the PS chains. On the basis of the global dimensions of the PS chains, evaluated by viscosity and LS experiments, suitable colloid contents were selected in order to perform supplementary SANS experiments on PS chains in DMF with OHSil. SANS experiments were performed with two different settings: (i) deuterated polystyrene chains (D8-PS) in hydrogenated DMF and in the presence of hydrogenated OHSil colloids give access to the PS form factor; (ii) deuterated PS (D8-PS) in deuterated DMF in the presence of hydrogenated OHSil colloids offer a chance to directly investigate the depletion zones generated by the single chains.

Experimental Details and Data Evaluation

Preparation of Hydroxy-Functionalized Silica Particles (OHSil) (Figure 1**).** OHSil is prepared according to a procedure developed by Mori et al.[23−25] At first, *N*,*N*-di(2,3-dihydroxypropyl)aminopropyltriethoxysilane has to be synthesized. Therefore, 3.34 g of glycidol (Acros, Geel, Belgium, technical grade) is added slowly to 5 g of 3-aminopropyltriethoxysilane (ABCR, Karlsruhe, Germany) while stirring. The mixture turns slightly yellow, and the viscosity increases dramatically. The mixture is kept at room temperature and stirred overnight. Completeness of the reaction is established by means of the educt peaks of the corresponding ^{13}C NMR spectrum between 25 and 55 ppm. The spectroscopic data of the hydroxy-functionalized silane read: ^{13}C NMR (125 MHz, $CDCl_3$) δ 69.8, 69.3 (CHOH); 64.9, 64.8 (CH_2OH); 58.5, 58.2 (NCH_2); 58.5, 58.4 (OCH_2); 57.8, 57.0 (NCH_2CHOH); 19.7, 19.6($CH_2CH_2CH_2$); 18.3, 18.2(CH_3); 7.8, 7.7 ($SiCH_2$). ^{29}Si NMR (60 MHz, $CDCl_3$) δ −45.15, −45.27. IR (KBr, cm^{-1}) 3375, 2976, 2928, 2875, 1640, 1442, 1394, 1298, 1144, 1043, 942, 721.

Second, 5 g of *N*,*N*-di(2,3-dihydroxypropyl)aminopropyltriethoxysilane in 16 g of methanol (technical grade) is added to 0.7 mL of 4% HF aqueous solution (diluted from 38 to 40%

Table 1. Characteristic Parameters of Linear PS Chains Used in Mixing Experiments[a]

PS sample	$M_w \times 10^{-3}$ [g/mol]	R_g [nm]	R_h [nm]	$A_2 \times 10^4$ [mol mL g^{-2}]
PS-2.5M	2602	63	45	1.61
PS-600K	613	30	20	1.58
D8-PS-600K	513	28	19	2.03

[a] M_w, R_g, A_2, and R_h are determined with light scattering experiments in DMF at 25 °C. All values are obtained by extrapolating to zero PS concentration.

HF, Merck, Darmstadt, Germany) in a polyethylene flask. The mixture is stirred for 4 h and kept overnight at room temperature. Larger particles are removed by means of a centrifuge (Hettich Zentrifuge, type 2001, EBA 8S) rotating for 1 h at 5000 rpm. Only the supernatant liquid is used for further processing, leaving the larger particles in the sediment. Excess water and methanol is removed by using a rotary evaporator under reduced pressure at 40 °C and 240 mbar and by successive application of a high vacuum for a few seconds. Application of a longer period of high vacuum has to be avoided due to an inevitable cleavage of ethanol and succeeding aggregation of particles. The highly viscous, yellow fluid is immediately dissolved in dimethylformamide. ^{29}Si NMR data (125 MHz, D_2O) read: δ −63.49, −63.46, −64.59, −66.05, −66.79, −68.04.

The OHSil concentrations c_C are calculated by weighting the obtained product and dissolving it in a certain amount of the desired solvent. Concentrations of OHSil are given in g/L. Since it is impossible to determine the amount of residual solvent in the product, OHSil concentrations c_C suffer from an uncertainty of roughly 10%. Therefore, quantitative comparison of concentration values can only be performed within batches.

Linear Polymer Chains. Linear polystyrene (PS) chains are purchased from Polymer Standards Service (Mainz, Germany). The behavior of PS chains in solution is investigated in the presence of different amounts of OHSil by means of viscosimetry, light scattering, and small-angle neutron scattering. In the latter case, fully deuterated PS samples are used. Characteristic parameters of all PS samples applied are summarized in Table 1.

Colloid−Solvent Systems for PS Chain Characterization. Two solvent systems are chosen to investigate PS chains in the presence of OHSil: pure dimethylformamide at 25 °C (DMF) and a mixture of DMF (70 vol %) and toluene (30 vol %) at 40 °C, from now on referred to as DMF−Tol. Toluene (Merck) is distilled prior to use; DMF (Acros) is stored over molecular sieves under an argon atmosphere. DMF−Tol at 40 °C is considered to be isorefractive to OHSil. An increase of the toluene fraction would enhance the isorefractivity but has to be discarded due to the insolubility of OHSil in nonpolar solvents.

Spectroscopy. NMR spectra are recorded on Bruker instruments (AMX 300 and AMX 500). Chemical shifts are reported in ppm from tetramethylsilane. IR spectra are recorded on a Bruker Equinox 55 instrument.

Refractive Index Measurements. Measurements are performed at room temperature with a scanning interferometric refractometer (Nanofilm Technology, Göttingen, Germany) operating at a wavelength of 543.5 nm. The measuring cell has a volume of 6.2 μL. Usually, the index of refraction n is measured for six or more concentrations c. The slope of a plot n vs c leads to the respective refractive index increment.

Density Measurements. To calculate dynamic viscosities according to eq 2, densities of the respective liquids are required. They are determined with a vibrating tube densitometer (Paar Digitale Präzisionsdichte-Messeinrichtung, DMA 02 D). The apparatus is controlled by a thermostat (Lauda, Germany) with a precision of ±0.1 K. The resonance frequency of the tube is specified by the mass of the tube plus the mass of the fluid inside. For each sample the resonance frequency is measured 10 times. The densitometer is calibrated with water and air as fluid systems with known densities.

Density measurements of OHSil solutions are carried out in DMF and DMF−Tol. In both cases a linear dependence of the density on OHSil concentration can be observed. Table 2 gives the parameters a and b of the linear equation

$$\rho = ac_{OHSil} + b \tag{1}$$

with ρ being the density and c_C the OHSil concentration in g/L.

Characterization of different OHSil batches indicates that colloid samples with reproducible molecular parameters and physical properties are synthesized. As an example, ρ according to eq 1 is evaluated in DMF for OHSil-14 in addition to OHSil-11. The resulting concentration dependence is ρ [kg/m^3] = 942.69 + 0.2529c_C, in good agreement with the relationship for OHSil-11 in DMF shown in Table 2. Thus, if not otherwise mentioned, the concentration dependence of ρ on OHSil concentration is based on OHSil-11 in DMF and on OHSil-8 in DMF-Tol.

Density measurements are also performed with solutions of deuterated PS in DMF in order to determine the partial specific volume of deuterated PS therein. The partial specific volume is required to calculate the appropriate neutron scattering contrast of deuterated PS according to eq 15. Therefore, a dilution series of D8-PS-600K in DMF at 25 °C is investigated, and the slope of a plot ρ vs c in g/L leads to the desired value.

Viscosity Measurements. In the present work, dynamic viscosities of OHSil solutions, established by means of eqs 1 and 2, are measured for the following purposes: (i) characterization of OHSil in solution by means of intrinsic viscosities requires $\eta_{solution}$; (ii) transformation of diffusion coefficients of PS chains from dynamic light scattering into hydrodynamically effective radii R_h in CP mixtures requires respective viscosities of the OHSil solutions.

Dynamic viscosities are measured using a typical Ostwald capillary viscometer (Schott Geräte, Hofheim a.Ts., Germany). The capillary is thermally adjusted in a water bath by a thermostat (Lauda, Germany) with a precision of ±0.1 K. For each concentration the time needed for a predefined volume to flow through the capillary is measured five times. After application of Hagenbach's correction, the corrected averaged flow times $\bar{t}$ are directly related[26] to the dynamic viscosity η.

$$\eta = K\rho\bar{t} \tag{2}$$

In eq 2, K is a viscometer constant, determined by calibrating the viscometer with five fluids, and ρ is the density of the investigated solutions determined according to eq 1. It should be mentioned that K and ρ are temperature dependent.

Intrinsic Viscosities. Characterization of OHSil colloids and of PS chains in CP mixtures proceeds as follows. Dilution series of both OHSil and PS chains consisting of at least five concentrations are measured in the respective solvent. The solvent is DMF in the case of OHSil and OHSil solutions in the case of PS. Extrapolating reduced viscosities $|\eta|$

$$|\eta| \equiv \frac{\eta_{solution} - \eta_{solvent}}{c\eta_{solvent}} \tag{3}$$

to zero concentration leads to the intrinsic viscosity $[\eta]$ according to

$$|\eta| = [\eta] + mc \tag{4}$$

All solvent parameters for the evaluation of viscosity experiments and light scattering data are summarized in Table 3.

Light Scattering Experiments of the OHSil Colloids. A first characterization of the OHSil colloids by light scattering was performed immediately after preparation in the original reaction medium methanol. Analysis of the electric field−time correlation function was based on Laplace inversion according to the CONTIN procedure.[27] As can be seen in Figure 2, two peaks are discernible. The peak with the lower averaged hydrodynamic radius corresponds to the desired product and

Table 2. Density and Viscosity of OHSil Solutions in DMF and DMF−Tol at Different Temperatures Used for the Investigation of PS in CP Mixtures[a]

parameter	batch no.	DMF (25 °C)	DMF−Tol (40 °C)
density ρ [kg/m^3]	OHSil-11	$943.59 + 0.2389c_C$	
viscosity η [Pa s]	OHSil-11	$7.550 \times 10^{-4} + 4.25 \times 10^{-6}c_C$	
fitted regime [g/L]		$0 < c_C < 160$	
density ρ [kg/m^3]	OHSil-8		$908.35 + 0.2611c$
viscosity η [Pa s]	OHSil-8		$6.095 \times 10^{-4} + 3.47 \times 10^{-6}c$
fitted regime [g/L]			$0 < c_C < 200$

[a] The OHSil concentration c_C is given in g/L.

Table 3. Solvent Properties Used in Viscosimetry and Light Scattering Experiments

solvent	T [°C]	ρ [g/mL]	η [mPa s]	n[39,40]	$(dn/dc)_{PS}$ [mL/g] at 25 °C
toluene	25	0.862	0.557[40]	1.496	0.103 (D8-PS)
DMF	25	0.943	0.794[40]	1.431	0.165[41]
DMF−Tol	40	0.908	0.610	1.451	0.149
methanol	25		0.567	1.326	

Table 4. Hydrodynamic Radii R_h of the Different OHSil Batches Determined by Analyzing the Correlation Functions at $\theta = 30°$[a]

batch no.	R_h [nm]	PDI	solvent (temp, °C)	concn for DLS c_C [g/L]	expts on CP
OHSil-5[b]	1.3	1.6	methanol (25)		
OHSil-8[c]	1.0		DMF−Tol (40)	88	
OHSil-10	1.1		DMF−Tol (40)	89	SLS/DLS
OHSil-11	1.4		DMF (25)	81	SLS/DLS
OHSil-12			DMF (25)		$[\eta]$
OHSil-14			DMF (25)		$[\eta]$[d]
OHSil-16	1.4	1.2	DMF (25)	103	SANS

[a] In the case where the particles are characterized directly after their synthesis, no absolute concentrations can be given. [b] Characterized in the original reaction medium after centrifugation. [c] Batch OHSil-8 is used to determine the viscosity and density relationship of OHSil in DMF−Tol. [d] In the case of experiments with PS-600K in the presence of OHSil-14, direct use was made of appropriate densities of OHSil-14 solutions.

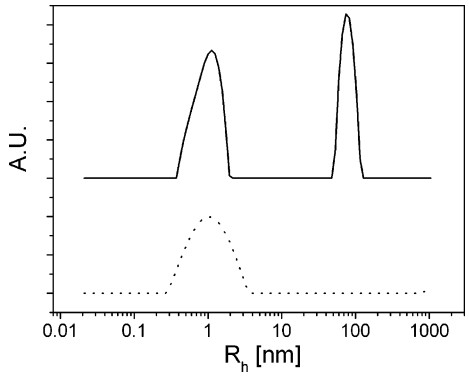

Figure 2. Results of CONTIN analysis from DLS measurements of OHSil-5 solutions in methanol at $\theta = 30°$ and $T = 25$ °C directly after particle formation where no absolute particle concentrations can be given. The top curve shows the result of the reaction solution without any purification steps. The bottom curve denotes the results after centrifugation. Comparison of both curves demonstrates the successful removing of larger particles.

the component with the larger radius stems from an irreversibly formed agglomerate. By centrifugation, a supernatant solution with the small colloids can be separated, leaving the undesired large particles in the sediment. The colloid sizes of all other OHSil batches are determined directly in the CP mixtures. Accordingly, hydrodynamic radii of OHSil are calculated from the particle fraction with the lower size. Results of the particle characterizations are given in Table 4. Different solvents are chosen due to their respective use in CP mixtures. Polydispersities of the small OHSil colloids, expressed in terms of the ratio of the weight-averaged particle mass to the number-averaged particle mass, covered a regime of $M_w/M_n = 1.4 \pm 0.2$. Polydispersities are estimated by means of a cumulant analysis.[28]

Light Scattering Experiments of PS in CP Mixtures. All scattering experiments are performed with a model 5000e compact goniometer system from ALV-Laser Vertriebsgesellschaft (Langen, Germany), which permits the simultaneous recording of static and dynamic light scattering. A Nd:YAG laser with 100 mW operating at a wavelength of 532 nm is used as a light source. Cylindrical quartz glass cuvettes with an outer diameter of 20 mm serve as scattering cells. The scattering intensity is observed in an angular range of 30°−150°. The cell housing is thermally adjusted by a thermostat (Haake, Germany) with a precision of ±0.01 K. All samples are filtered through PTFE syringe filters (Macherey-Nagel, Düren, Germany). For solutions containing PS chains with $M_w > 1\,000\,000$ g/mol a pore size of 0.45 μm is applied. In the case of all other solutions and solvents, filters with a pore size of 0.2 μm are used.

Light scattering experiments are carried out to investigate the conformation of PS chains in DMF and DMF−Tol at different concentrations of OHSil. At each OHSil concentration five PS concentrations are measured to allow extrapolation to infinite dilution. If represented according to Zimm's approximation,[29a] the static light scattering (SLS) data read

$$\frac{Kc}{\Delta R_\theta} = \frac{1}{M_W P(q)} + 2A_2 c \tag{5}$$

with M_W the weight-averaged molecular weight, $P(q)$ the form factor, A_2 the second osmotic virial coefficient, c the polymer concentration in g/L, and ΔR_θ the net scattering of the PS chains expressed in terms of the Rayleigh ratio. The contrast factor K is defined as

$$K = \frac{4\pi^2}{\lambda_0^4 N_A}\left(n\,\frac{dn}{dc}\right)^2 \tag{6}$$

In eq 6, λ_0, N_A, n, and dn/dc are the laser wavelength in a vacuum, Avogadro's number, the refractive index of the solvent, and the refractive index increment of the polymer, respectively. Changes of n due to the addition of OHSil is negligible at all concentrations c_C applied in the present work. The scattering vector q is defined as

$$q = \frac{4\pi n}{\lambda_0}\sin\left(\frac{\theta}{2}\right) \tag{7}$$

with θ the scattering angle. For particles significantly smaller than the wavelength, $1/P(q)$ can be approximated by

$$\frac{1}{P(q)} \cong 1 + \frac{R_g^2}{3}q^2 \tag{8}$$

with R_g^2 being the z-averaged mean-square radius of gyration.

In the case of polymer chains under good solvent conditions, data from SLS experiments are preferably evaluated according to Berry's[29b] approximation

$$\sqrt{\frac{Kc}{\Delta R_\theta}} = \sqrt{\frac{1}{M_W}}\left[1 + A_2 M_W c + \frac{R_g^2 q^2}{6}\right] \tag{9}$$

Extrapolated values of R_g, M_w, and A_2 for all investigated PS samples are summarized in Table 1.

To guarantee dilute solution behavior of the PS chains, their concentration regime is kept below the so-called overlap concentration estimated according to eq 10

$$c^* = \frac{M_W}{\frac{4}{3}\pi R_g^3 N_A} \tag{10}$$

Since not even DMF−Tol represents a completely isorefractive system, relaxation times of the OHSil particles are observable in addition to the one of PS chains in most cases. Thus, the apparent diffusion coefficients of the PS chains are extracted individually by the CONTIN analysis[28] and extrapolated to zero scattering angle and to infinite dilution separately. In a second step, the resulting diffusion coefficients are transformed into hydrodynamically effective radii R_h via the Stokes−Einstein equation

$$R_h = \frac{kT}{6\pi\eta}\frac{1}{D} \tag{11}$$

with k being Boltzmann's constant, T the temperature, and η the solvent viscosity. Since OHSil solutions are used as solvents for the polymer chains, the viscosities of different OHSil concentrations have to be determined. Table 2 gives the relationship between viscosity and OHSil concentration as linear fits.

Small-Angle Neutron Scattering of PS in CP Mixtures. Measurements are performed at the high flux reactor of the Institut Laue−Langevin (ILL) in Grenoble, France. The small-angle neutron scattering instrument D11 is used. Scattering intensities are recorded with a two-dimensional position-sensitive ^{3}He detector, which consists of a matrix assembly of 64 × 64 cells each having an area of 1 cm^2. All samples are measured at 25 °C. The calibration standard (H_2O) is put in a Hellma cell of 1 mm path length, whereas the path lengths of the solutions D_S vary. In the case of the experiments in hydrated DMF D_S equals 1 mm, and in the case of those in deuterated DMF D_S is 5 mm. A broad regime of momentum transfer q of 1.8×10^{-3} Å^{-1} < q < 0.33 Å^{-1} is covered by combining a neutron wavelength of 6 Å with sample−detector distances of 1.1, 5, 10, and 34 m.

The transmission of the samples is determined by measuring the direct, attenuated beam (at $q = 0$) passing through any object (I_x), divided by the analogous measurement of the incident beam (I_i):

$$T_x = \frac{I_x(q=0)}{I_i(q=0)} \tag{12}$$

After determination of the central detector coordinates for each sample−detector distance, the two-dimensional raw data are radially averaged. Averaged data are transformed to differential cross sections per volume by use of the known wavelength-dependent effective values of H_2O (tabulated for D11 ^{3}He detector:[30] $d\Sigma/d\Omega_{H_2O} = 0.905$ cm^{-1} for $\lambda = 6$ Å).

The differential scattering cross section per unit volume of the solutions and the solvent are separately calculated according to the following equation:[31]

$$\left(\frac{d\Sigma}{d\Omega}\right)_S = \frac{(I_S - I_{Cd}) - \frac{T_{S+EC}(1 - n_S\tau)}{T_{EC}(1 - n_{EC}\tau)}(I_{EC} - I_{Cd})}{(I_{H_2O} - I_{Cd}) - \frac{T_{H_2O+EC}(1 - n_{H_2O}\tau)}{T_{EC}(1 - n_{EC}\tau)}(I_{EC} - I_{Cd})} \times \frac{T_{H_2O+EC}(1 - n_{H_2O}\tau)\cdot 0.1\left(\frac{d\Sigma}{d\Omega}\right)_{H_2O}}{T_{EC}(1 - n_{EC}\tau)D_S} \tag{13}$$

The indices denote sample (S), corresponding to solvents or solutions, standard (H_2O), empty cells (EC), and cadmium (Cd). The cadmium measurement provides the electronic background. The term $(1 - n\tau)$ takes into account the correction for dead time losses, with n being the integral count rate of each measurement and τ being the dead time.

All scattering experiments are performed with a fully deuterated PS sample denoted as D8-PS-600K (Table 1). Two types of experiment are performed. In one type of experiment, deuterated PS is dissolved in a solution of OHSil-16 colloids in DMF. A PS concentration of $c_{PS} = 2$ g/L is characterized at five different OHSil-16 concentrations corresponding to c_C = 0, 50, 93, 103, and 105 g/L. In one out of this set, $c_C = 50$ g/L, a full dilution series based on four different PS concentrations was characterized. In this case, an exact extrapolation of the scattering behavior to $c_{PS} = 0$ g/L became possible. The second type of experiment is an analogous series of scattering measurements at four concentrations of the sample D8-PS-600K in OHSil-16 solutions in deuterated DMF (from Deutero, Kastellaun, Germany), again at a concentration of $c_C = 50$ g/L. Replacement of DMF by deuterated DMF matches the contrast of the PS chains instead of the OHSil particles, and the interference pattern of the scattered neutrons now responds to the domains depleted from OHSil colloids due to the excluded-volume interaction with PS chains.

In both types of experiment, the net intensities of the D8-PS-600K samples were calculated according to

$$\Delta\left(\frac{d\Sigma}{d\Omega}\right)_{sample} = \left(\frac{d\Sigma}{d\Omega}\right)_{solution} - \left(\frac{d\Sigma}{d\Omega}\right)_{solvent} \tag{14}$$

The term $(d\Sigma/d\Omega)_{solvent}$ represents the background scattering from solvents, respectively. Depending on the type of experiment, the solvent is deuterated DMF, hydrogenated DMF, or OHSil in hydrogenated DMF. In the lattermost case $(d\Sigma/d\Omega)_{solvent}$ is explicitely recorded for c_C = 50, 93, and 103 g/L. Clear independence of all three curves from the OHSil content indicates successful contrast matching in hydrogenated DMF and allowed us to use the $(d\Sigma/d\Omega)_{solvent}$ recorded at $c_C = 103$ g/L also for the experiment at $c_C = 105$ g/L. The incoherent background scattering in eq 14 always stems from the D8-PS-600K chains only, which can be neglected.[31]

To calculate absolute molecular weights according to eq 9 from SANS data of the PS concentration series at $c_C = 50$ g/L, the neutron scattering contrast K_{SANS} has to be determined by applying eqs 15 and 16.

$$K_{SANS} = (L_2^{coh} - L_1^{coh}\rho_1 v_2)/N_A \tag{15}$$

$$L_k^{coh} = \sum_\alpha^{n_A} b_\alpha N_A/M_k \tag{16}$$

The index k denotes the type of molecule (1 = solvent; 2 = monomer). The remaining symbols read as follows: ρ_1 density of the solvent, v_2 the partial specific volume of the polymer sample in DMF, b_α the coherent scattering lengths of all n_A atoms given in Table 5, and M_k the molecular mass of the solvent or the monomer. v_2 is determined for D8-PS-600K in DMF at 25 °C to 0.645 mL/g via density measurements. Calculating the constant K_{SANS} for D8-PS in DMF leads to $K_{SANS} = 5.40 \times 10^{-3}$ cm^2 mol g^{-2}.

In the case of dilution series of D8-PS-600K at $c_C = 50$ g/L the concentrations vary from 1 g/L < c_{D8-PS} < 4 g/L, leading

Table 5. Coherent Scattering Lengths for Different Nuclei[42]

nucleus	b [10−12 cm]	nucleus	b [10−12 cm]
H	−0.374	O	0.581
D	0.667	N	0.939
C	0.665		

to intensities increasing considerably in quality with larger c_{D8-PS}. This enables analysis of the low-q regime to be based on the extrapolation toward zero concentration and scattering vector of four different scattering curves. In the case of single PS concentration experiments a Berry analysis of the low-q regime (3.08×10^{-3} Å $< q < 4.94 \times 10^{-3}$ Å) according to eq 9 leads to results of low significance. This is due to the low scattering intensities at the largest detector distance. Therefore, only the form factor fits covering a wider q regime are used for data evaluation in the experiments at variable c_C concentration and a single D8-PS-600K concentration of $c_{D8-PS} = 2$ g/L. Experimental uncertainties forced us to neglect q values lower than 3.08×10^{-3} Å for extrapolations to $c_{PS} = 0$ g/L.

Results and Discussion

On the Nature of the OHSil Colloids. All OHSil batches used as colloid component in CP mixtures were characterized by DLS. The results are summarized in Table 4. All colloids exhibit the same size within experimental uncertainty. As is illustrated with OHSil-5 in Figure 2, the size distribution of OHSil is quite broad, corresponding to polydispersity indices between 1.2 and 1.6.

Although the absolute concentration of the OHSil solutions are not exactly known, it is possible to get a first guess of their molecular weight by static light scattering. To this end, explicit experiments were performed with one sample, OHSil-11. The refractive index increment of the batch OHSil-11 has been determined to 0.037 mL/g in DMF at room temperature. Since the particles are very small, no angular dependent scattering is observed, and the analysis of one scattering angle is sufficient. For the same reason, the influence of the second osmotic virial coefficient can be neglected, and eq 5 simplifies to

$$\frac{Kc}{\Delta R_\theta} = \frac{1}{M_W} \tag{5b}$$

leading to a molecular weight of the OHSil-11 batch at 25 °C of ∼4000 g/mol. The corresponding value for the hydrodynamically effective radius is 1.4 nm.

Viscosity experiments were performed in addition to the characterization by light scattering. According to Einstein,[32] the viscosity of a solution of an ideal hard sphere only depends on the volume fraction Φ occupied by the spheres irrespective of their size. He found

$$\eta_{solution} = \eta_{solvent}(1 + 2.5\Phi) \tag{17}$$

where Φ is the volume fraction calculated as follows

$$\Phi = \frac{4\pi {R_C}^3 c_C N_A}{3M} \tag{18}$$

with c_C being the concentration in g/L, N_A Avogadro's number, and M and R_C the molar mass and the radius of the respective spheres. The factor $4\pi {R_C}^3/3$ is the hydrodynamically effective volume of the dissolved particles, which in the case of ideal spheres corresponds to the sphere volume. If a particle radius of 1.2 nm

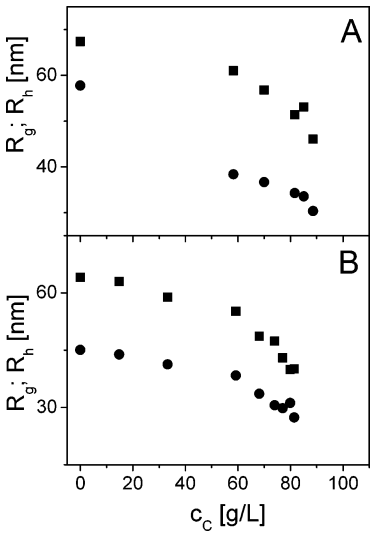

Figure 3. Radii of gyration R_g and hydrodynamically effective radii R_h from light scattering for the sample PS-2.5M in dilute solution at variable concentration of OHSil. (A) PS in the presence of OHSil-10 in DMF−Tol at 40 °C. The density and viscosity relationships for OHSil-10 solutions are approximated by the fits of OHSil-8 given in Table 2. (B) Experiments with OHSil-11 in DMF at 25 °C. The symbols in (A) and (B) denote the following: R_g (■), R_h (●).

averaged over all batches, is used, an alternative estimation of the molecular weight of OHSil is possible according to the following procedure.

Under the assumption that the OHSil particles behave like ideal hard spheres, their reduced viscosity should be independent of the OHSil concentration, corresponding to $m = 0$ in eq 4. This is in fact observed. Inserting eq 18 into eq 17 and eq 17 into eq 3 leads to

$$\frac{4\pi {R_C}^3 N_A}{3} = [\eta]\frac{M}{2.5} \tag{19}$$

Use of the intrinsic viscosity of 3 mL/g results in a molecular weight of 3600 g/mol. This value is in fair agreement with the value obtained by static light scattering and indicates an almost quantitative removal of solvent residues during the preparation. Together with an average colloid density of $\rho = 3M_W/4\pi {R_h}^3 N_A = 0.83$ g/mL, which is fairly large, this confirms the suitability of the OHSil particles to act as the colloid component in CP mixtures at the protein limit.

Global Dimensions of PS Chains in OHSil Solutions. Three methods have been applied to investigate the size of the PS chains: viscosimetry, light scattering, and SANS. The present section will focus on the first two methods, where dilution series of PS chains had been examined in DMF and DMF−Tol in order to enable extrapolation to infinite dilution of PS chains. Both solvents act as good solvents for the PS chains. Results are summarized in Figures 3 and 4.

Light scattering measurements were performed with PS-2.5M chains having a molar mass of 2600 kDa. In both solvents, the radius of gyration and the hydrodynamic radius decrease with increasing content of OHSil colloids. Data points to a collapse transition of the PS chains occurring at an OHSil concentration around 100 g/L. If this limit is crossed, the phase turns instable. At this point, we have to emphasize that only in DMF−Tol a satisfactory index matching of the colloids is achieved, and the light scattering signal can be

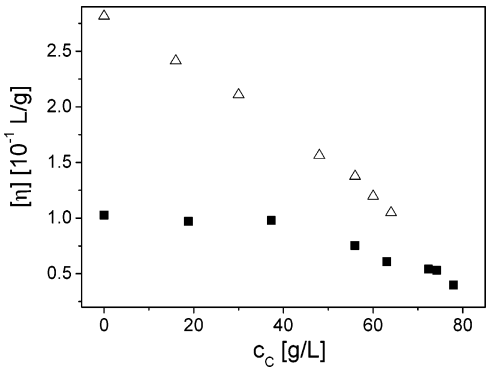

Figure 4. Intrinsic viscosities of PS in DMF at 25°C at variable concentrations of OHSil: PS-600K with OHSil-14 (■); PS-2.5M with OHSil-12 (Δ). The sample PS-600K has a similar molar mass as the deuterated PS sample D8-PS-600K used for all SANS experiments.

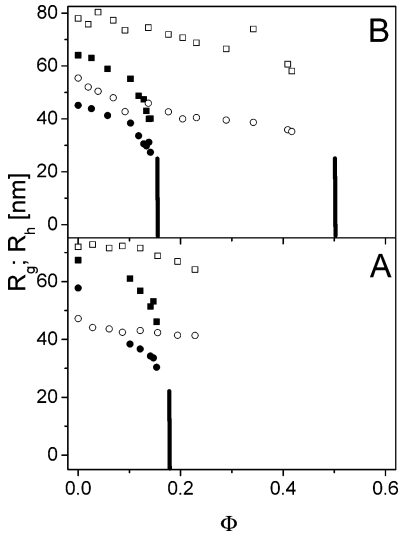

Figure 5. Chain dimensions of PS-2.5M expressed as R_g und R_h vs the volume fraction Φ of OHSil (eq 16) and of SILS (ref 22). (A) corresponds to isorefractive colloid−solvent systems: R_g (□) and R_h (○) for SILS in toluenel/ethyl acetate (50 vol %/50 vol %) at 40 °C (ref 22); R_g (■) and R_h (●) for OHSil-10 in DMF−Tol at 40 °C. (B) R_g (□) and R_h (○) for SILS in toluene at 25 °C (ref 22); R_g (■) and R_h (●) for OHSil-11 in DMF at 25 °C. Vertical bars indicate the onset of macroscopic phase separation.

attributed unambiguously to the PS chains. Yet, the decrease of the hydrodynamically effective volume of the PS chains, independently demonstrated by intrinsic viscosity measurements for two different PS samples in the nonisorefractive colloid−solvent system (Figure 4), supports the OHSil-induced coil collapse in both solvents. Therefore, we are able to confirm the effect of coil shrinking induced in the protein limit by SILS molecules[22] now with different colloid−solvent systems.

Noticeably, the size of OHSil particles is roughly twice as large as the SILS molecules. Neglecting a possible impact of slight chemical differences between OHSil and SILS on the interaction with PS chains, this may offer a chance to illustrate the influence of colloid size on the PS chain shrinking and phase behavior in PS−colloid mixtures. Such a comparison greatly benefits from the fact that the same PS sample (PS-2.5M) has been used in both colloid−polymer systems. Details are outlined in Figure 5, which compares directly the trend of PS radii at variable OHSil volume fraction (this work) and of SILS particles (ref 22). Obviously, an increase of the

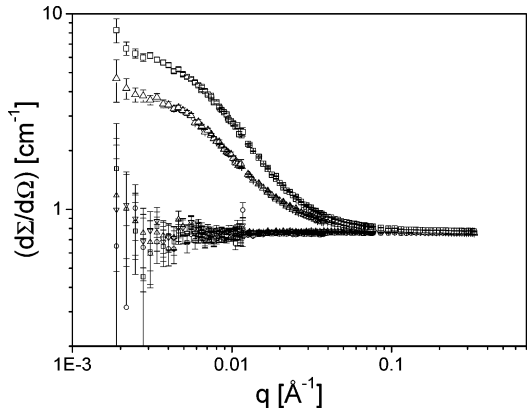

Figure 6. Neutron scattering curves of OHSil-16 solutions in DMF at variable concentrations of OHSil-16 [0 g/L (□); 50 g/L (○); 93 g/L (Δ); 103 g/L (▽)] in comparison to neutron scattering curves of two D8-PS-600K solutions with c_{PS} = 2 g/L: experiment in pure DMF corresponding to c_C = 0 g/L (Δ) and in an OHSil-16 solution with c_C = 103 g/L (□).

colloid size causes the volume fraction of colloids where a chain collapse and a phase separation may take place to decrease from Φ ∼ 0.5 to 0.17, in qualitative agreement with predictions by van der Schoot[13] and Bolhuis et al.[16]

The molar mass values for the PS chains measured by SLS at variable OHSil concentrations exhibit two different tendencies. In DMF−Tol, which is almost isorefractive to OHSil, the apparent mass values of PS are independent of the OHSil content, and in DMF it decreased with increasing OHSil content (ref 33).

SANS Experiments. All SANS experiments were performed with the fully deuterated PS sample D8-PS-600K. This enabled us to illuminate CP mixtures from two different perspectives: (i) by using deuterated DMF as the solvent, the PS chains are fully matched leaving the OHSil particles as the only scatterers; (ii) if regular DMF is used, the situation is reversed, making form factors of the PS chains accessible. Although both perspectives have been adopted in the present work, the main focus lies on the evaluation of the single-chain behavior as a function of the OHSil concentration. Feasibility of this route is demonstrated by means of Figure 6, which includes scattering curves of D8-PS-600K in pure DMF and in an OHSil solution with c_C = 103 g/L together with the corresponding solvents, which are pure hydrogenated DMF and OHSil solutions in hydrogenated DMF. The latter curves show neither an angular dependence nor a variation with the OHSil concentration, thus clearly demonstrating that the OHSil particles could successfully be matched by hydrogenated DMF. Curves of D8-PS-600K in OHSil solutions in hydrogenated DMF therefore can unambiguously be attributed to the PS chains. In the case of c_C = 103 g/L the curve is slightly higher than the respective curve in pure hydrogenated DMF. Both curves were recorded at the same PS concentration. Thus, the small difference can unambiguously be attributed to an interparticular excluded-volume effect of PS, which obviously is less pronounced if OHSil particles are present additionally in solution.

In a first series of scattering experiments two corresponding sets of PS concentrations were investigated at an OHSil concentration of 50 g/L. In one set, the contrast of OHSil particles was fully matched by regular DMF, and in the other set, the deuterated PS chains were made "invisible" by using deuterated DMF. Each

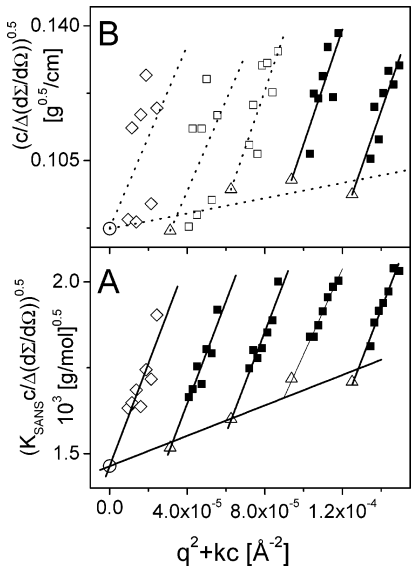

Figure 7. Zimm diagrams of D8-PS-600K with c_{PS} = 1, 2, 3, and 4 g/L in OHSil-16 solutions with c_C = 50 g/L. Experiments in diagram A are performed in hydrogenated DMF, yielding the following apparent radii of gyration R_g: 24.3 nm (c_{PS} = 1 g/L); 23.5 nm (c_{PS} = 2 g/L); 20.9 nm (c_{PS} = 3 g/L); 22.8 nm (c_{PS} = 4 g/L). The value at infinite dilution is R_g = 24.7 nm. Experiments in diagram B are performed in deuterated DMF, yielding the following apparent radii of gyration R_g for the two highest concentrations: 29.9 nm (c_{PS} = 3 g/L) and 30.1 nm (c_{PS} = 4 g/L). Experimental uncertainty of data at lower concentrations forbids quantitative evaluation of the respective parameters, and the dotted lines are used as guide for the eye only.

set exhibits a dependence of the scattering behavior on the D8-PS-600K concentration. Both sets are based on the same four PS concentrations which cover the dilute concentration regime.

Results are compared in Figure 7. Precision of the scattering data in the case of fully matched OHSil particles was good enough to allow for a conventional Zimm analysis of the scattering behavior of the PS chains (Figure 7A). Extrapolation to zero concentration revealed a molar mass of 470 000 g/mol, a second virial coefficient of 0.98×10^{-4} mol mL g^{-2}, and a mean-square radius of gyration of R_g = 24.7 nm. The molar mass is in good agreement with LS data. Remarkably, the second virial coefficient decreased by a factor of 2, indicating the onset of a screening of a polymer−polymer interactions due to OHSil particles.

Scattering signals of the reversed situation with the PS chains fully matched (Figure 7B) also reveal a structural feature related to the PS chains, although it has to be fully attributed to the OHSil particles. Unfortunately, the lower quality of data excludes an extrapolation to zero PS concentration in this case. However, evaluation of the apparent radii of gyration became possible at the two highest PS concentrations. Comparison of the resulting R_g values (29.9 and 30.1 nm) with the two respective R_g values of the PS chains in Figure 7A (20.9 and 22.8 nm) indicates size correlations of comparable order of magnitude in both cases but a significantly lower absolute size value in the case of the PS chains. Two results can be extracted. In the case of fully matched PS chains the discernible structure can be related to zones depleted from OHSil particles caused by the "invisible" PS chains. The absolute values indicate depleted zones which are larger than the radius of gyration of the PS chains.

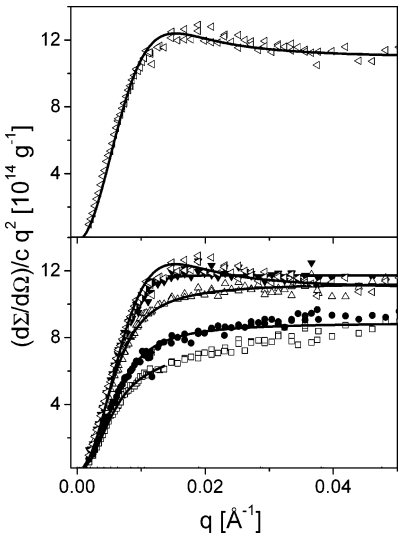

Figure 8. Kratky plots of D8-PS-600K with c_{PS} = 2 g/L in hydrogenated DMF at variable contents of OHSil-16. The symbols indicate the following OHSil concentrations: c_C = 0 g/L (□) [expanded coil[34]]; c_C = 50 g/L (●) [Gaussian coil[35]]; c_C = 93 g/L (△) [Gaussian coil[35]]; c_C = 103 g/L (▼) [3-arm star[36,37]]; c_C = 105 g/L (tilted △) [4-arm star[36,37]] shown in the upper and lower figure. The chain models mentioned in square brackets indicate the model leading to the best fit, respectively. Supplementary information for the fits is shown in Figure 9.

Finally, a series of D8-PS-600K solutions were investigated at variable contents of OHSil particles. To this end, solutions at a constant concentration of c_{PS} = 2 g/L were prepared in hydrogenated DMF at five different OHSil contents corresponding to c_C = 0, 50, 93, 103, and 105 g/L. The regime of OHSil concentrations of 0 g/L ≤ c_C ≤ 105 g/L was based on preceding light scattering data with the same system, which suggest a precipitation threshold close to c_C = 109 g/L.

Figure 8 compares all five scattering curves by means of a Kratky plot. Comparison is performed by using differential scattering cross sections per unit volume dΣ/dΩ of the PS chains directly because they all refer to the same concentration of PS. The experimental curve recorded in pure DMF could be described by the model of an excluded-volume chain derived by Utiyama et al.[34] With increasing OHSil content, data increasingly exceed the behavior observed at c_C = 0 g/L. Qualitatively spoken, this deviation corresponds to a weakening of the decay of the form factor with increasing amounts of OHSil which can be clearly interpreted as a coil contraction induced by the presence of OHSil particles. Quantitative description of such systems is difficult because no theoretical model curves for contracted linear chains are yet available. At this point we have to emphasize that the same trend has already been demonstrated with a chemically different system in the protein limit.[21] In that case, small poly(ethyl methacrylate) (PEMA) colloids were mixed with deuterated PS chains in toluene. The resulting scattering curves of the PS chains indicated a decrease of chain dimensions with increasing content of PEMA colloids. Although branching could be definitely excluded as a model, the coil contraction induced by the PEMA colloids led to changes of the form factor and thus the density−density correlation function which is comparable to changes along a transformation of a corresponding linear Gaussian chain into a regularly branched star.[21]

In transferring this argument to the present system, we performed curve fittings of the scattering curves

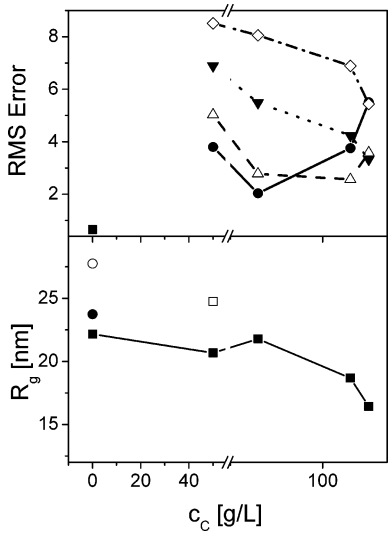

Figure 9. (A) Root-mean-square deviations of the experimental data from model curves. The model curves result from the respective least-squares fits shown in Figure 8. The fits were performed in a regime of momentum transfer of 0.00189 Å^{-1} < q < 0.0136 Å^{-1} in the case of an expanded coil[34] and of 0.00189 Å^{-1} < q < 0.05 Å^{-1} in all other cases.[35−37] The symbols denote expanded coil (■), Gaussian coil (●), 3-arm star (△), 4-arm star (▼), and 5-arm star (◇). (B) Radii of gyration of D8-PS-600K in DMF and in DMF with OHSil. Open symbols result from full Zimm anlysis of the SLS experiment in pure DMF (○) and of the SANS experiment at c_C = 50 g/L (□). Full symbols indicate apparent radii, determined at a finite PS concentration of 2 g/L by means of model fits to SANS curves presented in Figure 8 (■) and by means of SLS (●).

recorded at 50, 93, 103, and 105 g/L with theoretical calculations on linear Gaussian chains[35] and regularly branched Gaussian stars.[36] All formulas for form factors used in fits are summarized in the Appendix. Each of the four experimental curves is fitted with four theoretical curves, a Gaussian linear chain, a 3-arm star, a 4-arm star, and a 5-arm star. The fit parameter is the radius of gyration. The quality of all four fits can be evaluated by means of the root-mean-square deviation (rms) of the data points from the fit.

The rms values of the fits are summarized in Figure 9. In the case of c_C = 50 g/L the linear Gaussian chain provides the most accurate description of the experimental data. At c_C = 93 g/L, as the next higher colloid content, the situation did not change much, except for the fact that the rms value for the fit with the 3-arm star also improved and comes closer to the value for the Gaussian chain one. It is only at c_C = 103 g/L when the sequence begins to inverse. Now the 3-arm star describes the situation best, followed by a linear chain and a 4-arm star with the latter leading to equal results. At the highest colloid content, it is the 4-arm star which revealed the best fit, closely succeeded by the 3-arm star. The 4-arm star is the star with the lowest number of arms exhibiting a maximum in the Kratky plot as the most striking feature of regularly branched structures. This fit behavior was expected because the experimental curve at the highest colloid content also exhibits a shallow maximum.[37]

Consistency of the fit results can be evaluated by a discussion of the resulting radii of gyration and together with the lengths of the appertaining Gaussian monomer and by comparison with the data from D8-PS-600K in pure DMF, which corresponds to a polymer chain under good solvent condition and which represents a reference system. Representation of the respective data in Figure 9 demonstrates a significant shrinking of the coil dimensions with increasing OHSil concentration in the first place. However, we have to be aware of the fact that the radii are apparent in nature because they are extracted at finite concentrations. This can best be illustrated at c_C = 0 g/L where the extrapolated value is known independently from light scattering together with the respective apparent value at c_{PS} = 2 g/L. In line with expectations, both apparent values, from SANS and SLS, are lower than the extrapolated R_g due to the influence of the second osmotic virial coefficient on the angular scattering. However, shrinking of the chains with increasing OHSil concentrations indicates a decreasing excluded volume effect. The latter could independently be demonstrated by a comparison of A_2 values measured at c_C = 0 g/L and c_C = 50 g/L, which exhibited a decrease from 2 × 10^{-4} to 1 × 10^{-4} mol mL/g^{-2}, respectively. Excluded-volume effects eventually become negligible for c_C > 50 g/L. The radius of gyration of R_g = 16.4 nm at c_C = 105 g/L can then be used to estimate a shrinking ratio by comparison with the unperturbed dimensions of the respective chain $R_g(\Theta)$ estimated to be R_g = 22.5 nm from experiments at c_C = 50 or 93 g/L

$$R_g(c_C = 105\ \text{g/L})/R_g(\Theta) = 16.4/22.5 = 0.73 \quad (20)$$

The value of 0.73 is close to the shrinking ratio $\sqrt{g} = \sqrt{(3f - 2)/f^2} = 0.79$ predicted for regularly branched Gaussian chains[38] if the number of arms f equals 4. Comparison of R_g = 16.4 nm with R_g = 28.9 nm as the original or reference value (good solvent conditions, c_C = 0 g/L) indicates a shrinking by almost a factor of 0.5.

The consistency of the fits performed with the particle scattering factors on Gaussian linear chains and regular stars can be independently confirmed by a closer look on the resulting lengths of the corresponding Gaussian monomer l_k. Using a contour length of $L = M_W/m_l$ for D8-PS-600K, which is calculated from the molecular mass and the length of a styrene monomer (m_l = 450 g mol^{-1} nm^{-1}), a value for l_k can be estimated according to

$$R_g^2 = \frac{Ll_k}{6}\frac{3f - 2}{f^2} \quad (21)$$

The resulting values are l_k = 2.32 nm (f = 1, c_C = 50 g/L), l_k = 2.37 nm (f = 3, c_C = 103 g/L), and l_k = 2.26 nm (f = 4, c_C = 105 g/L). All values agree, indicating that consistent fits could be achieved with a unique number of Gaussian segments $N = L/l_k$.

Summary

On the basis of a procedure suggested by Mori et al.,[24,25] we prepared small OHSil particles with an average radius of 1.2 nm. In combining these particles with PS chains with a radius of gyration of 30 nm, colloid−polymer mixtures in solution became accessible, which perfectly fit into the protein limit. These achievements allowed us to investigate the chain dimensions of PS as a function of the OHSil concentration in two different solvents. Combined light scattering and viscosity experiments revealed shrinking dimensions with increasing OHSil concentrations in both solvents, one of which is isorefractive with the OHSil colloids. Noteworthy, the OHSil volume fraction which caused the

largest extent of shrinking and which lay close to the phase boundary of the CP was ~1.7. This critical volume fraction, being found in the presence of the OHSil particles, is significantly lower than the respective volume fraction observed earlier in the presence of the smaller SILS particles.[22] Thus, we could for the first time present experimental evidence for a qualitative prediction of a correlation between colloid size and phase boundary given by van der Schoot.[13] In the following step, extended SANS experiments were performed with deuterated PS chains in DMF. To this end an appropriate series of OHSil concentrations were selected, covering the one phase regime up to the phase boundary. In deuterated DMF, with the PS chains fully matched, we could demonstrate the existence of a zone depleted of OHSil particles. The size of this zone was larger than the corresponding radius of gyration of the PS chains. In hydrogenated DMF, the only scatterers left are the PS chains, giving direct access to changes of the chain dimensions induced by an increasing amount of OHSil colloids. In line with the light scattering and viscosity experiments, the chains revealed a considerable compaction, once the phase boundary was approached. At this boundary, scattering curves could be successfully described by form factors of regularly branched structures. Obviously, chain compaction due to the addition of small colloids leads to similar changes of the density−density correlation functions within the PS chains as cutting the same chain into arms equal in length and reconnecting the arms to a central unit as a regular star. Together with earlier experiments on chemically different CP in the protein limit,[21,22] chain shrinking of polymers under good solvent conditions caused by the presence of appropriate amounts of small colloids can now be considered a general property of CP mixtures in the protein limit.

Acknowledgment. The work greatly benefited from valuable discussions with P. van der Schoot, Dutch Polymer Institute. We thank Lukas Kurtze for his skillful experimental support of our synthetic efforts. This work is supported by the Deutsche Forschungsgemeinschaft, project HU 807/5-1.

Appendix

Form Factor of an Expanded Coil. Utiyama et al.[34] calculated an expression for the scattering behavior of flexible polymer coils under good solvent conditions. The equation

$$P(q) = 2\sum_{i=0}^{\infty}\frac{(-1)^i\Gamma[(2i+l+1)/t]y^{2i}}{(2i+1)![1+i(1+\epsilon)][2+i(1+\epsilon)]\Gamma[(l+1)/t)} \quad \text{(A1)}$$

with

$$y^2 = \frac{\Gamma[(l+1)/t]}{\Gamma[(l+3)/t]}(2+\epsilon)(3+\epsilon)q^2{R_g}^2$$

$$t = 2/(1-\epsilon)$$

is valid in the regime of $(qR_g)^2 < 10$, corresponding to 0.00189 Å^{-1} < q < 0.0136 Å^{-1} in the case of D8-PS-600K under present consideration. On the basis of a recommendation by Utiyama et al.,[34] the fit was performed with $\epsilon = 0.18$ and with $l = 2.7$.

Gaussian Chain Models. Linear flexible chains are described by the linear Gaussian chain model[35]

$$P(q) = \frac{2}{q^4{R_g}^4}[\exp(-q^2{R_g}^2) - (1 - q^2{R_g}^2)] \quad \text{(A2)}$$

Theoretical form factors of regular stars with f Gaussian arms are described by[38]

$$P(q) = \frac{2}{fV^2}\left[V - (1 - \exp(-V)) + \frac{f-1}{2}(1 - \exp(-V))^2\right] \quad \text{(A3)}$$

with

$$V = \frac{f}{3f-2}q^2{R_g}^2$$

Equations A2 and A3 are used to fit the experimental data in a regime of 0.00189 Å^{-1} < q < 0.05 Å^{-1}.

References and Notes

(1) Asakura, S.; Oosawa, F. *J. Chem. Phys.* **1954**, *22*, 1255. Asakura, S.; Oosawa, F. *J. Polym. Sci.* **1958**, *33*, 183.
(2) Vrij, A. *Pure Appl. Chem.* **1976**, *48*, 471.
(3) Poon, W. C. K. *J. Phys.: Condens. Matter* **2002**, *14*, R859.
(4) Tuinier, R.; Rieger, J.; de Kruif, C. G. *Adv. Colloid Interface Sci.* **2003**, *103*, 1.
(5) Walter, H.; Brooks, D. E. *FEBS Lett.* **1995**, *361*, 135.
(6) Murphy, L. D.; Zimmermann, S. B. *Biophys. Chem.* **1995**, *57*, 71.
(7) Tuinier, R.; Dhont, J. K. G.; de Kruif, C. G. *Langmuir* **2000**, *16*, 1497.
(8) de Gennes, P. G. *C. R. Acad. Sci. B* **1979**, *288*, 359.
(9) Schaink, H. M.; Smit, J. A. M. *J. Chem. Phys.* **1997**, *107*, 1004.
(10) Sear, R. P. *Phys. Rev. E* **2002**, *66*, 51401−1.
(11) Shaw, M. R.; Thirumlai, D. *Phys. Rev. A* **1991**, *44*, R4797.
(12) Sear, R. P. *Phys. Rev. E* **1998**, *58*, 724.
(13) van der Schoot, P. *Macromolecules* **1998**, *31*, 4635.
(14) Odijk, T. *Biophys. Chem.* **1998**, *73*, 23.
(15) Odijk, T. *Physica A* **2000**, *278*, 347.
(16) Bolhuis, P. G.; Meijer, E. J.; Louis, A. A. *Phys. Rev. Lett.* **2003**, *90*, 068304.
(17) Dijkstra, M.; Frenkel, D. *Phys. Rev. Lett.* **1994**, *72*, 298.
(18) Luna-Bárcenas, G.; Bennett, G. E.; Sanchez, I. C.; Johnston, K. P. *J. Chem. Phys.* **1996**, *104*, 9971.
(19) Zherenkova, L. V.; Mologin, D. A.; Khalatur, P. G.; Kkokhlov, A. R. *Colloid Polym. Sci.* **1998**, *276*, 753.
(20) Kramer, T.; Scholz, S.; Maskos, M.; Huber, K. *J. Colloid Interface Sci.* **2004**, *279*, 447.
(21) Kramer, T.; Schweins, R.; Huber, K. *J. Chem. Phys.* **2005**, *123*, 014903.
(22) Kramer, T.; Schweins, R.; Huber, K. *Macromolecules* **2005**, *38*, 151.
(23) Mori, H.; M. G.; Müller, A. H. E.; Klee, J. E. *J. Am. Chem. Soc.* **2003**, *125*, 3712.
(24) Mori, H.; Lanzendörfer, M. G.; Müller, A. H. E.; Klee, J. E. *Macromolecules* **2004**, *37*, 5228.
(25) Mori, H.; Lanzendörfer, M. G.; Müller, A. H. E.; Klee, J. E. *Langmuir* **2004**, *20*, 1934.
(26) *Manuel Jakubith, Grundoperationen und chemische Reaktionstechnik*; Wiley-VCH: Weinheim, 1998.
(27) Provencher, S. W. *Comput. Phys.* **1982**, *272*, 13, 229.
(28) Koppel, D. E. *J. Chem. Phys.* **1972**, *57*, 4818.
(29) (a) Zimm, B. H. *J. Chem. Phys.* **1948**, *16*, 1093. (b) Berry, G. C. *J. Chem. Phys.* **1966**, *44*, 4550.
(30) Lindner, P. *J. Appl. Crystallogr.* **2000**, *33*, 807.
(31) Lindner, P. In *Neutrons, X-rays and Light: Scattering Methods Applied to Soft Condensed Matter*; Lindner, P., Zemb, Th., Eds.; Elsevier: Amsterdam, 2002; p 23.
(32) Einstein, A. *Ann. Phys.* **1911**, *33*, 591.
(33) The refractive index increments of SILS molecules as the colloid component (ref 22) differ in sign from the refractive index increments of PS in the nonisorefractive solvent, causing the apparent molar mass of the PS chains to increase with increasing SILS content. In the case of OHSil in DMF,

a residual positive refractive index increment having the same sign as the one for PS reversed the trend observed for PS in SILS.
(34) Utiyama, H.; Tsunashima, Y.; Kurata, M. *J. Chem. Phys.* **1971**, *55*, 3133.
(35) Debye, P. *J. Chem. Phys.* **1946**, *14*, 636.
(36) Benoit, H. *J. Polym. Sci.* **1953**, *11*, 507.
(37) Burchard, W. *Macromolecules* **1977**, *10*, 919.
(38) Stockmayer, W. H.; Fixmann, M. *Ann. N.Y. Acad. Sci.* **1953**, *57*, 334.
(39) *Landolt-Börnstein*; Springer: Berlin, Vol. III/38A.
(40) *CRC Handbook of Chemistry and Physics*; CRC Press: Boca Raton, FL, 1993.
(41) Brandrup, J. *Polymer Handbook*, 3rd ed.; John Wiley: New York, 1996.
(42) Bee, M. *Quasielastic Neutron Scattering: Principles and Applications in Solid State Chemistry, Biology and Materials Science*; Bristol, 1988.

MA051308J